International Journal of Mechanical, Industrial and Aerospace Sciences
ISSN: 2517-9950
Vol:12, No:4, 2018

# Experimental and Simulation Stress Strain Comparison of Hot Single Point Incremental Forming

Amar Al-Obaidi,Verena Kräusel, Dirk Landgrebe

***Abstract*—**Induction assisted single point incremental forming (IASPIF) is a flexible method and can be simply utilized to form a high strength alloys. Due to the interaction between the mechanical and thermal properties during IASPIF an evaluation for the process is necessary to be performed analytically. Therefore, a numerical simulation was carried out in this paper. The numerical analysis was operated at both room and elevated temperatures then compared with experimental results. Fully coupled dynamic temperature displacement explicit analysis was used to simulated the hot single point incremental forming. The numerical analysis was indicating that during hot single point incremental forming were a combination between complicated compression, tension and shear stresses. As a result, the equivalent plastic strain was increased excessively by rising both the formed part depth and the heating temperature during forming. Whereas, the forming forces were decreased from 5 kN at room temperature to 0.95 kN at elevated temperature. The simulation shows that the maximum true strain was occurred in the stretching zone which was the same as in experiment.

***Keywords*—**Induction heating, single point incremental forming, FE modeling, advanced high strength steel.

## I. Introduction

THE single point incremental forming (SPIF) technique permits making complex sculpted shapes from sheet metal instead of applying a complicated, costly, specific punchs. SPIF is currently can be considered as an advanced sheet metal forming process and was innovated at adequate production costs to shape the high-strength metals. Furthermore, the application of hot single point incremental forming (HSPIF) process, in order to improve formability, gained a lot of interest by many researchers. Laser was used to heat up a sheet of titanium [1] the utilization of two synchronized devices was described: a robot to move and hold the punch to form the sheet and a locating device that was used to move and hold the heating source. In contrast, [2] used only a single device at which a CNC milling machine that forms the workpiece and a laser that acts as the heat source. An assembled system was fixed on the CNC machine that guides the laser beam and contains optics and mirrors. In another research investigation, a heating device was used [3]; an electrical current was utilized to heat the sheet during forming. The forming punch was connected to a robot. At the same time, a second punch connected to another robot was used to support the sheet. As a result, the researchers discovered high wear rates in the forming punch.

Conventional sheet metal forming proceses like bending, deep drawing and spinning were used to form the High strength steels into specified forms by using complicated punch designs. These methods contributed to the high cost of accessories when neglecting the mass production factor. Furthermore, applying temperature is not easily performed when using conventional methods [4], compared to the utilization of a laser or an electrical current in (HSPIF) for the prototype production. In fact, elevated temperatures contribute significantly to enhance the formability of hard to form metals by increasing ductility.

A high wear of the forming punch was discovered [3] and [5] during heating with a DC current. Moreover, 2.5 mm was reduced from the forming punch length during SPIF assisted by resistance heating of DC04 steel [6]. In the same way, heating by laser was limited to the beam spot diameter. Furthermore, some other limitations in heating by laser, considering the high cost and the operation and must be isolated for safety purposes. Early researches concentrated on heating up and forming the sheet blank at no more than 650 °C. The sheet metal of DP980 steel was heated by induction on the bottom side, and forming was conducted by a hemispherical punch at the upper side of the sheet metal [7]. Certainly the homogeneity of thickness distribution of the formed wall thickness was effected by the heating temperature. Therefore, an accurate investigation to calculate analytically and experimentally the thickness reduction for the formed wall thickness was not carried out for HSPIF.

The first HSPIF simulation was investigated by [8] the simulation model set up temperature was increased for the whole model. The processed method in theoretical view is not acceptable because of it considers that the overall sheet, punch and the clamping fixture were heated to elevated temperature. However, the suggested IASPIF experiment in this paper is depend only on local heating. Another HSPIF simulation [9] was carried to simulate the effect of heat on the stresses propagated during forming. The formed region was divided into three areas at first bending then shear at the end reverse bending. A real comparison between the experimental

V. Kräusel is with the Institute of Machine Tools and Production Processes IWP, Technische Universität Chemnitz, Chemnitz, Germany, Professorship of Forming and Joining UFF.

A. Al-Obaidi is with the Institute of Machine Tools and Production Processes IWP, Technische Universität Chemnitz, Chemnitz, Germany, Professorship of Forming and Joining UFF (corresponding author, e-mail: amar-baker-salim.al-obaidi@s2013.tu-chemnitz.de, phone: +49 371 531-34693).

D. Landgrebe, Fraunhofer-Institute for Machine Tools and Forming Technology IWU, Chemnitz, Germany (e-mail: dirk.landgrebe@iwu.fraunhofer.de).

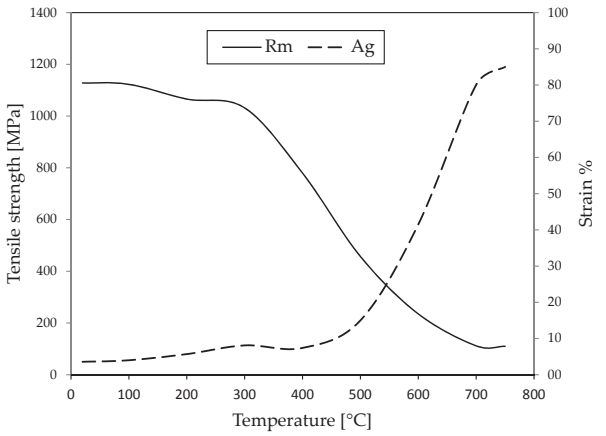


Fig. 1 The heating temperature effect on the mechanical properties of DP980 steel, Rm: maximum tensile strength [MPa] and Ag: elongation percentage

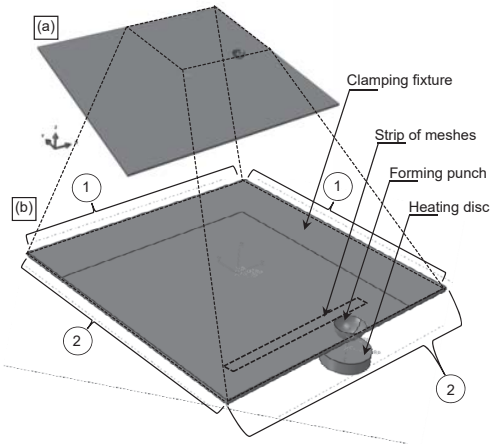


Fig. 2 Simulation model (a) full sheet and (b) quarter sheet at which 1 and 2 are encastre fixed and symmetric boundary conditions respectively

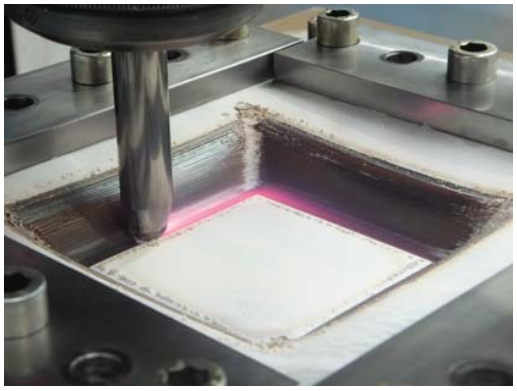

Fig. 3 IASPIF process during pyramid profile forming and induction heating

and analytical forming forces is necessary to understand the thinning that occurred in the formed wall part.

## II. Methodology

Abaqus CAE program was dependent as a finite element simulation program to simulate the SPIF process. The plastic properties of the DP980 steel sheet metal were extracted from the tensile test. Whereas, the tensile strength for the samples were tested in different temperatures from room temperature to 750 °C. The forming curves were calculated from the previous tensile tests to use it in the metal mechanical plastic properties for the Abaqus program model. Fig. 1 is showing the effect of heat on the elongation and tensile strength of the tested sheet metal. These tests were achieve by heating the DP980 steel to the required temperature with soaking time up to 20 minutes for the tensile test samples, after that tension was performed. The tensile tests were done according to DIN EN 10002-5. A universal tensile testing machine inspect 150 kN manufactured by (Hegewald & Peschke) GmbH was applied in the experiments. The heating oven was attached to the testing machine and the temperature was applied during the tensile test process.

The SPIF simulation was well known by the huge time requirements to analyze the deformation process. As many researchers preferred to simulate only a pie model in the circular formed parts, like only 45° pie [10]. Anisotropy of the material is not considered in the analyzed model and the isotropic von Mises yield criterion was depended.

A quarter of 75 × 75 mm from the 150 × 150 mm sheet was taken in the simulation to decrease the nodes number and the simulation time as shown in Fig. 2. In addition, a symmetry boundary condition was considered for simulating the quarter portion that was taken from the whole model. Furthermore, three layers were investigated in the sheet model and a strip of meshes was selected to record the various mechanical and thermal behavior of sheet metal after forming. The simulation profile was of 62° pyramid wall angle formed from 1.2 mm thickness of DP980 steel.

The induction power utilized in the experiment was 15 kW. In addition, the induction power supplied from a generator of high frequency (140-350 kHz) and maximum 50 kW capacity made by ELDEC Schwenk Induction GmbH. A fully explained details of the IASPIF experimental process can be found in [11] and the process can be seen in Fig. 3. The formed shape part in the experiment was formed with 62 ° wall angle from 1.2 mm thickness sheet of DP980 steel as shown in Fig. 4.

### A. Forming Forces at Room Temperature

The difference between the simulation and experimental SPIF forming forces in z-axis direction (Fz) were represented in Fig. 5. In addition, both simulation and experimental Fz curves at which their signals were smoothed by Lowess method [12]. The highest force values were not exactly matched this is due to the large iteration in the force values besides the smoothing of the force signals. However, the two curves were showing some similar slop in curvature. Consequently, the simulation model curve was approached to the real experiments curve for the given DP980 steel.

Fig. 4 Pyramid of DP980 steel and 1.2 mm thickness formed by IASPIF process of 62° wall angle

Moreover, as indicated in the investigations performed by Bouffioux [13] there is no 100 % real similar identical values between the simulation and the experimental force results.

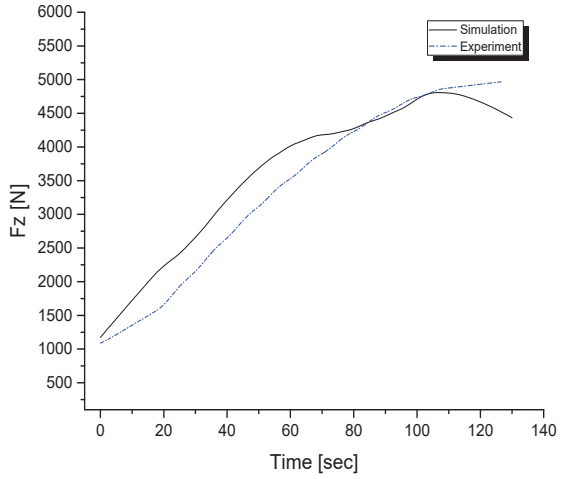


Fig. 5 Comparison between the simulation and experiment Fz at room temperature

### B. Fully Coupled Simulation Analysis

This method simplified by applying a coupled dynamic, temperature displacement, explicit step analysis. This process was accomplished by forming on the upper side of the sheet via forming punch. On the other hand, the heat was generated by a circular heating disk that moves in the lower side of the sheet as shown in Fig. 2. The heat was transferred from the heating disk to the sheet during forming. The sheet was heated locally by this method at which the heating disc was following the forming punch by applying the same path for both of them.

The mesh elements applied in the sheet were of three-dimensional solid elements, brick-shape eight-node C3D8T thermally coupled brick trilinear displacement. These mesh elements were well known by their capability to simulate the heat transfer with displacement due to the high calculation accuracy. In other words, the brick element type was used because of the capability to simulate the through-thickness

TABLE I
HSPIF PARAMETERS ALL DIMENSIONS IN MM

| IASPIF and sheet metal parameters | | | |
|---|---|---|---|
| Wall angle[°] | 62 | Sheet thickness | 1.2 |
| Feed rate [mm/min] | 2000 | Incremental step | 0.5 |
| Profile | pyramid | Coefficient of friction | 0.128 |
| Sheet metal | DP980 | dis. | 2 |
| Sheet conductivity | 54 W/m K | Punch diameter | 8 |
| Heating disc parameters | | | |
| Disc metal | copper | Thickness | 4 |
| Conductivity | 385 W/m K | Diameter | 20 |

deformation that occurred in the SPIF method. Furthermore, the capability of the brick element to deform uniformly during SPIF process. The SPIF is well known by a high plastic strain values. The punch and heating disc were considered as rigid nondeformable elements. The simulation parameters that used in the simulation and in the experiment are shown in Table I. The distance between the induction coil and the sheet (dis.) was 2 mm in the IASPIF experiment the same dis. was dependent between the sheet and the heating disc during simulation.

### C. Stresses Resulted from the Simulation

The proposed investigated model is to simulate the resulted formed mechanical properties indicating that the stresses were reduced and a potential increase has occurred in the plastic strains. In order to extract the simulation thermal stresses and strains number of nodes were selected in the 15 sec from the simulation time as presented in Fig. 6. These nodes were presenting the surrounding circumference of the forming punch except that the node number 1 where it was located at the center of the punch. The nodes 2, 5 and 7 were located after the forming punch in order to record the stresses and strains after forming. In the same time, the nodes 4, 6 and 9 are before the punch and the nodes 3 and 8 were located on the right and the left sides respectively of the punch. In addition, besides the nodes in the punch side layer which was called processing layer another nine nodes were considered on the lower side that located in the third layer and called unprocessing layer. Moreover, the unprocessing nodes were extinguished by a dash symbol from $\acute{1}$ to $\acute{9}$.

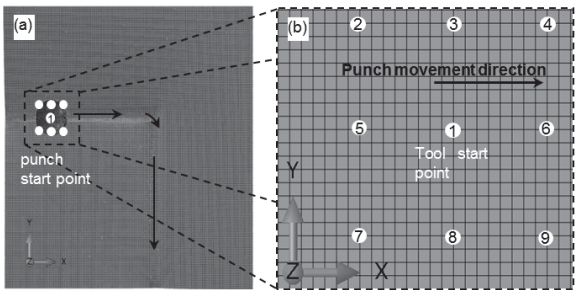


Fig. 6 Coupled simulation model (a) punch movement direction during forming and (b) enlarged view of the punch position showing the 9 nodes location

The stresses initiated during the analyses as shown in Table II were indicated that when the punch is penetrated in the

sheet at the nodes number 1 and 1́ the stresses distribution are quite complex. The stresses were shear, compressive and tensile stresses showing that the HSPIF simulation process is within a high iteration of the huge difference in stress values. A pure fully tensile stress was found near the punch end after forming because of the tensile stresses in three directions at the nodes 2, 5 and 7. In the same time, the largest stresses are presented on both sides at nodes 6 and 6́ in y-axis direction due to the punch acceleration during movement. Moreover, the tensile stresses appeared in all directions at nodes 4 and 5.

At which:

$\sigma_x$ = Stress in x-axis direction [Mpa].
$\sigma_y$ = Stress in y-axis direction [Mpa].
$\sigma_z$ = Stress in z-axis direction [Mpa].
$\tau_{xy}$ = Shear stress in the in x-axis and y-axis plan [Mpa].
$\tau_{xz}$ = Shear stress in the in x-axis and z-axis plan [Mpa].
$\tau_{yz}$ = Shear stress in the in y-axis and z-axis plan [Mpa].

TABLE II
STRESSES OF THE NODES ON THE SHEET AT 70 SEC TIME FROM THE TOTAL TIME OF 140 SEC

| Node no. | $\sigma_x$ | $\sigma_y$ | $\sigma_z$ | $\tau_{xy}$ | $\tau_{xz}$ | $\tau_{yz}$ |
|---|---|---|---|---|---|---|
| Processed side of the sheet | | | | | | |
| 1 | -81.5 | -71.9 | -85.7 | -2.76 | -47.2 | 16 |
| 2 | 44.4 | 47.6 | 1.03 | -58.3 | -10.9 | 5.79 |
| 3 | -29.5 | 90.6 | 9.61 | -12.7 | -2.25 | 16.6 |
| 4 | 26.1 | 84.3 | 11.5 | 49.3 | 12.3 | 12.5 |
| 5 | 80.2 | 9.37 | 4.51 | -1.72 | 1.06 | 3.69 |
| 6 | 39.6 | 12 | -2.08 | 3.28 | 8.31 | 24.3 |
| 7 | 63.4 | 31.2 | 3.17 | 57.3 | -7.43 | -0.538 |
| 8 | -63.4 | 55.3 | -0.996 | 17.4 | -8.03 | -16.9 |
| 9 | 12.8 | 74.7 | 2.08 | -50.5 | 8.45 | -4.06 |
| Unprocessed side of the sheet | | | | | | |
| 1́ | 25 | 43 | -25 | 18 | -37 | 25 |
| 2́ | -36 | -26 | 2 | 62 | 2 | 1.05 |
| 3́ | 51 | -7 | -0.491 | 23 | 3 | 0.096 |
| 4́ | 24 | -21 | 2.105 | -61 | -2 | 0.465 |
| 5́ | -74 | 43 | -1.8 | 23 | -0.795 | -5 |
| 6́ | -8 | 9.8 | 6 | -27 | 5 | -6 |
| 7́ | -52 | 6 | -2 | -56 | -5 | -6 |
| 8́ | 68 | -43 | -1.02 | -30 | -3 | -13 |
| 9́ | 19 | 18 | -1.026 | 63 | 6 | -5 |

The most nodes at the unprocessed sheet side were experiencing compressive stresses in most directions due to the punch pressing on the sheet through movement. It is worth to note that the location of the maximum principle tensile strength ($\sigma_{ts}$) was appeared in the same location where located also the maximum principle true strain (PE) as presented in Fig. 7. Moreover, the Von Mises stress was always appeared under the punch.

### D. Equivalent Plastic Strain

A strip of meshes was taken from the HSPIF simulation model to sense the results in a topographical expression. The strip of meshes is clearly located in the sheet as observed in Fig. 7. Furthermore, the strip of meshes as indicated in Fig. 2 before forming was well formed. An interesting result from the coupled HSPIF simulation as demonstrated in Fig. 8 where the maximum equivalent plastic strain (PEEQ) values

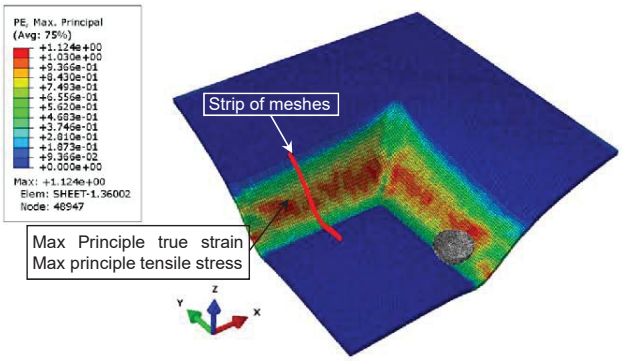


Fig. 7 Simulation deformed pyramid showing the strip of meshes

were located in the pyramid corner edge. Therefore, the both compression and tension forces action were taking place as listed by Martins [14]. The tabulated increase of PEEQ value was related to the development in simulation time that leads to the rise in pyramid depth. This was indicated by the strip of meshes as shown in Fig. 8 (b). The PEEQ value is considered as the ability of the metal to be formed and it is considered an indication of the forming degree.

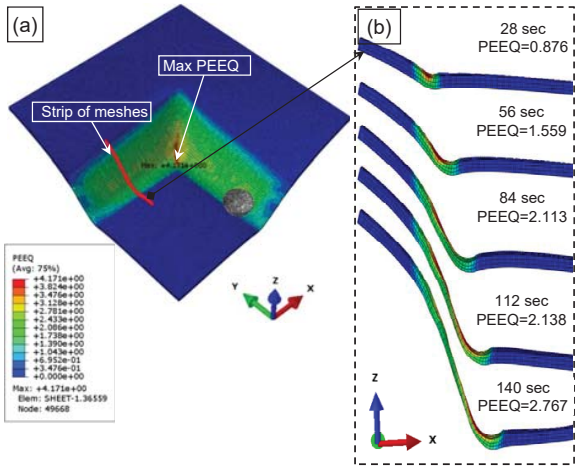


Fig. 8 Simulation deformed pyramid (a): deformed model showing the location of the PEEQ values at 900 K, (b): cut strip of meshes from (a) illustrating the development of PEEQ values with forming time

### E. The Effect of Increasing the Simulation Heating Temperature

Four simulation models were utilized to investigate the effect of local heating analyses; the first one was performed at room temperature. In the same time, the rest three models were operated in 900 K, 1000 K and 1100 K as a heating temperature for the heating disc. Fig. 9 demonstrates the reduction of stress components when the heating temperature is raised especially in the 1100 K model. The PE was also highly influenced by the simulation model temperature. Therefore, the PE was increased from 0.203 at 293 K to 1.02334 1100 K. In addition, the extreme development in the PEEQ values was presented clearly in Fig. 9. Moreover, the electric single point incremental forming simulation that was

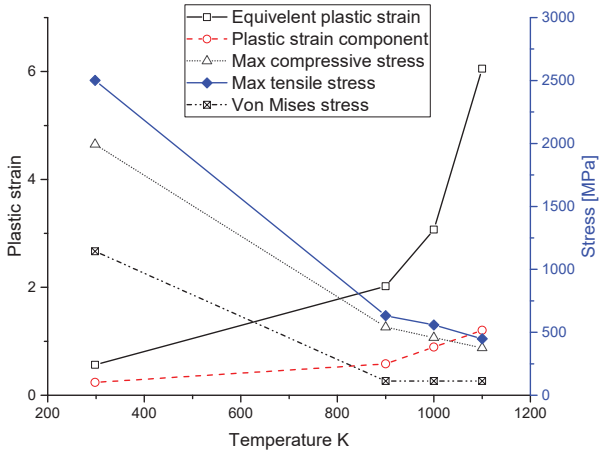


Fig. 9 The influence of heating temperature on the stress strain components for pyramid of DP980 steel

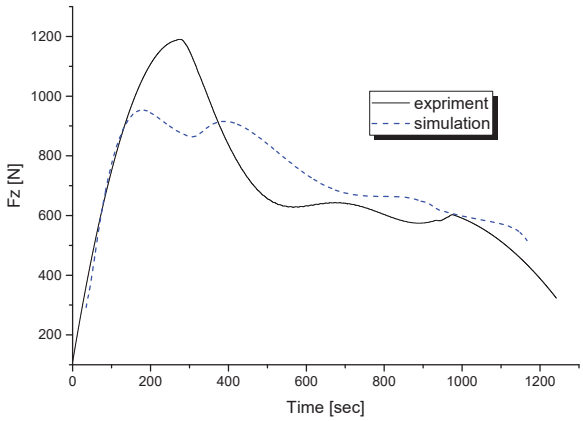


Fig. 10 Comparison between the simulation and experiment forces in z-axis

investigated by Fan [9] found the highest PEEQ value was also in the pyramid corner.

## III. Comparison between the Simulation and Experiment Results

The simulation process by Abaqus program was represented the forces and true strains in the z-axis direction compared with those measured in experiment during the IASPIF process. A list of results presented by forming forces and produced wall part thickness during forming.

### A. Forming Forces

Fig. 10 is highlighting the difference between the results of simulation and experiment forces in the z-axis direction. These results were concluded by smoothing the forming force values. The propagation of both simulation and experiment force values are closed to be identical at the start of the forming process. Due to the penetration and forward movement of the punch in the sheet this similarity has appeared. Furthermore, as the hot forming proceeded a disagreement was presented between the simulation and experiment force values. This difference was rising owing to the continuous deformation of sheet metal by the punch leads to make a variation in the heat losses between the simulation and experiment forces. Besides the heat difference between the simulation and experiment results, another major reason was appeared. The yield criterion applied was von Mises in the simulation. Whereas, in experiment the material was exhibiting another plastic anisotropy during IASPIF. Finally, the proposed coefficient of friction between the punch and the sheet may be not the exact one because of the appearance of heat variance during hot forming. Moreover, the homogeneity in the heating temperature distribution of both simulation and experiment in particular forming stages was illustrated Fig. 11.

The heating temperature of the IASPIF was measured by an IR camera during all the process experiment time. In addition, the simulation heating temperature was accomplished via the hot disc and recorded for all the simulation time. At which the maximum average difference in heating temperature $\Delta T$ was 60 K and 127 K between the simulation and experiment process stages respectively. It is worth to note that the same IASPIF parameters used to form the pyramid in Fig. 10 were also that used to measure the heating temperature in Fig. 11.

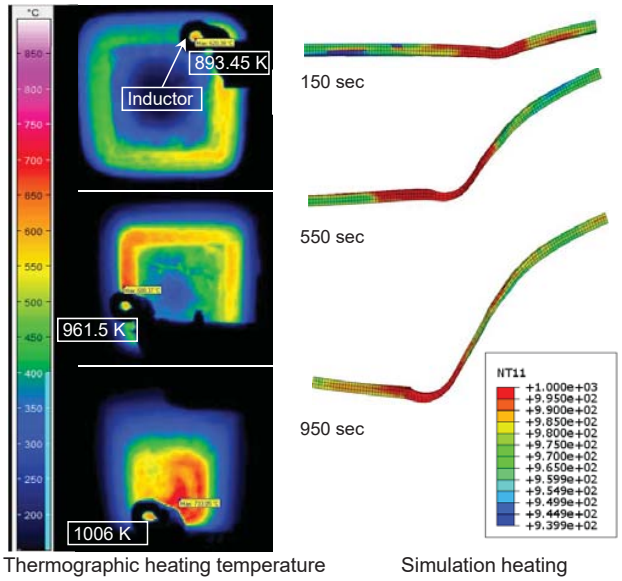


Fig. 11 Simulation and experiment heating temperature in the sheet at different forming times

The influence of the formed part geometrical depth through SPIF process was concluding the variation in forming forces. The variation of forming forces due to the change in heating temperature that occurred during laser SPIF simulation was also discovered by Mohammadi [15]. The difference between experiment and simulation forming forces owing to the extremely localized heating in the experiment. Whereas, the heat distribution in the simulation was not locally in the sheet like those in the experiment.

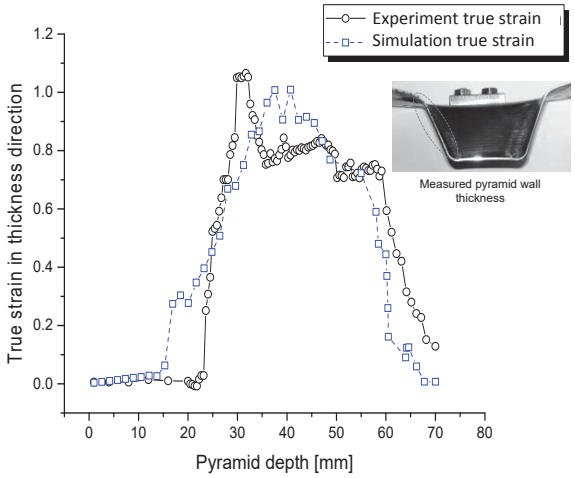


Fig. 12 Simulation and experiment true strain in thickness direction of 62° pyramid wall angle

### B. True Strain in Thickness Direction

The sheet metal during IASPIF was well stretched and a high local thinning occurred during the deformation process. Therefore, according to equation (1) the true strain values were calculated for the whole depth of the formed 62° wall angle pyramid.

$$\varepsilon_t = ln\frac{t_o}{t} \tag{1}$$

$\varepsilon_t$= strength coefficient
$t_o$= initial sheet thickness [mm]
$t$ = final sheet thickness [mm]

The results of true strain for both simulation and experiment are compared in Fig. 12. The maximum true strain values were 1.15 and 1.042 for experiment and simulation respectively. This rapprochement between true strain values is considered as a strong point in the validation of the proposed simulation. The three deviations of the formed wall part bending, shear and reverse bending as distinguished by Fan [9] presenting that the thinning was located in the shear area. As a result the excessive thinning of part thickness caused by stretching action in the shear area. A validation for the IASPIF process was experimented [16] showing that the forming by a fixed feed rate producing a nonhomogeneous distribution in the hardness of the formed wall part. Whereas, forming by a varied feed rate that increased during IASPIF resulting a homogeneous distribution in the hardness of the formed wall part.

## IV. Conclusion and Future Work

A simulation and experimental investigations were performed to analysis the behavior of DP980 sheet metal during HSPIF. The main results can be concluded:

- The difference between simulation and experiment in the Fz values during forming at room temperature was 4 %
- The HSPIF was done by heating the sheet during forming with a circular disc moves simultaneously with the forming punch
- The highest stresses in the z-axis was found and it was a compressive stress type
- PEEQ value was raised by increasing the formed part depth. In the same time, the PEEQ and PE were increased by increasing the heating temperature during forming the PE was increased from 0.203 at 293 K to 1.02334 1100 K
- Thinning of the formed wall angle was occurred at both experiment and simulation process due to the shear stress

Simulation of the real induction heating process coupled with SPIF process would be better to analysis the whole IASPIF. Furthermore, a simulation with a varied feed rate during IASPIF process and compare it with fixed feed rate results.

## Acknowledgment

The authors would like to thank the Institute of Machine punchs and Production Processes IWP at the TU Chemnitz and the Fraunhofer Institute for Machine punchs and Forming Technology IWU for their support.

## References

[1] J. Duflou, B. Callebaut, J. Verbert, and H. De Baerdemaeker, "Laser assisted incremental forming: formability and accuracy improvement," *CIRP Annals-Manufacturing Technology*, vol. 56, no. 1, pp. 273–276, 2007.
[2] A. Göttmann, J. Diettrich, G. Bergweiler, M. Bambach, G. Hirt, P. Loosen, and R. Poprawe, "Laser-assisted asymmetric incremental sheet forming of titanium sheet metal parts," *Production Engineering*, vol. 5, no. 3, pp. 263–271, 2011.
[3] H. Meier and C. Magnus, "Incremental sheet metal forming with direct resistance heating using two moving tools," in *Key Engineering Materials*, vol. 554. Trans Tech Publ, 2013, pp. 1362–1367.
[4] K. Mori, S. Maki, and Y. Tanaka, "Warm and hot stamping of ultra high tensile strength steel sheets using resistance heating," *CIRP Annals-Manufacturing Technology*, vol. 54, no. 1, pp. 209–212, 2005.
[5] G. Fan, F. Sun, X. Meng, L. Gao, and G. Tong, "Electric hot incremental forming of ti-6al-4v titanium sheet," *The International Journal of Advanced Manufacturing Technology*, vol. 49, no. 9, pp. 941–947, 2010.
[6] X. Shi, L. Gao, H. Khalatbari, Y. Xu, H. Wang, and L. Jin, "Electric hot incremental forming of low carbon steel sheet: accuracy improvement," *The International Journal of Advanced Manufacturing Technology*, vol. 68, no. 1-4, pp. 241–247, 2013.
[7] A. Al-Obaidi, V. Kräusel, and D. Landgrebe, "Hot single-point incremental forming assisted by induction heating," *The International Journal of Advanced Manufacturing Technology*, vol. 82, no. 5-8, pp. 1163–1171, 2016.
[8] S. Kim, Y. Lee, Y. Kwon, and J. Lee, "A study on warm incremental forming of az31 alloy sheet," *Transactions of Materials Processing*, vol. 17, no. 5, pp. 373–379, 2008.
[9] G. Fan and L. Gao, "Numerical simulation and experimental investigation to improve the dimensional accuracy in electric hot incremental forming of ti–6al–4v titanium sheet," *The International Journal of Advanced Manufacturing Technology*, vol. 72, no. 5-8, pp. 1133–1141, 2014.
[10] J. Belchior, L. Leotoing, D. Guines, E. Courteille, and P. Maurine, "A process/machine coupling approach: application to robotized incremental sheet forming," *Journal of Materials Processing Technology*, vol. 214, no. 8, pp. 1605–1616, 2014.
[11] A. Al-Obaidi, V. Kräusel, and D. Landgrebe, "Improvement of formability in single point incremental forming of dp1000 steel aided by induction heating." *Applied Mechanics & Materials*, vol. 794, 2015.
[12] H. P. William, A. T. Saul, T. V. William, and P. Flaneery Brian, *Numerical Recipes in C - The Art of Scientific Computing*. Cambridge University Press, 1992.
[13] C. Bouffioux, C. Lequesne, H. Vanhove, J. Duflou, P. Pouteau, L. Duchêne, and A. Habraken, "Experimental and numerical study of an almgsc sheet formed by an incremental process," *Journal of Materials Processing Technology*, vol. 211, no. 11, pp. 1684–1693, 2011.

[14] P. Martins, N. Bay, M. Skjødt, and M. Silva, "Theory of single point incremental forming," *CIRP Annals-Manufacturing Technology*, vol. 57, no. 1, pp. 247–252, 2008.
[15] A. Mohammadi, H. Vanhove, A. Van Bael, and J. R. Duflou, "Towards accuracy improvement in single point incremental forming of shallow parts formed under laser assisted conditions," *International Journal of Material Forming*, vol. 9, no. 3, pp. 339–351, 2016.
[16] A. Al-Obaidi, V. Kräusel, and D. Landgrebe, "Induction heating validation of dieless single-point incremental forming of ahss," *Journal of Manufacturing and Materials Processing*, vol. 1, no. 1, p. 5, 2017.